

Perfectly conducting channel on the dark surface of weak topological insulators

Yukinori Yoshimura¹, Akihiko Matsumoto¹, Yositake Takane¹, and Ken-Ichiro Imura¹

¹*Department of Quantum Matter, AdSM, Hiroshima University, Higashi-Hiroshima 739-8530, Japan*
(Dated: March 5, 2013)

A weak topological insulator (WTI) bears, generally, an even number of Dirac cones on its surface; they are susceptible of doubling, while on the surface of a certain orientation it shows no Dirac cone. On this “dark” surface of a WTI, we predict the existence of a single pair of isolated 1D perfectly conducting channels that forms either a closed loop or a segment of a line. The former is associated typically with a single atomic-layer-thick island formed on the dark surface, while the latter is shown to be the consequence of a pair of crystal (screw) dislocations terminating on the dark surface.

PACS numbers: 73.20.-r, 61.72.Lk, 73.22.-f

The specificity of the three-dimensional (3D) topological insulator is that it can be weak [1–3]. Initially, this weak topological phase has not been paid much attention under the pretext that it is not more than a mere adiabatic deformation of an ordinary insulator. Yet, it has later turned out that in this so-called weak phase a topological non-triviality is not actually weak but rather hidden [4, 5]. In contrast to its counter part, the strong topological insulator (STI), which exhibits a single protected Dirac cone, the weak topological insulator (WTI) bears either an even number or, depending on the way the crystal is cleaved, no gapless Dirac cone on its surface. And for this very reason, the WTI is often mistaken for possessing no robust topological character.

The topological non-triviality ensuring the emergence of gapless Dirac cones on the surface of topological insulators is encoded in its non-trivial or inverted band structure, that is to say, stems from a non-trivial feature in the reciprocal space. In a WTI at least one of the three so-called weak \mathbb{Z}_2 indices ν_1, ν_2, ν_3 [6] remains non-zero, reflecting its non-trivial band structure. The status of the STI and WTI could be inverted when this reciprocal-space feature is interconnected with a topologically non-trivial real-space character such as a dislocation of the crystalline structure in the real space. In the examples shown in Refs. [4, 7] a WTI exhibits a protected gapless state bound to such a dislocation, while this is not necessarily the case with STIs.

The real-space geometry, or the shape of the sample plays also an important role in the spectrum of the surface state [8]. Indeed, except for the case of an isolated infinitely large single surface, the surface state is not actually gapless in the strict sense; the gaplessness is not immune to finite-size gap opening. And the magnitude of this finite-size energy gap is qualitatively different in different geometries. In the simplest and most commonly used geometry of a slab such a finite-size energy gap is exponentially small, and may practically be negligible except in extremely thin film samples [9]. In prism-shaped (isomorphic to a cylinder, or a filled torus) [10–12] or cubic (spherical) [13] STI, the magnitude of the size gap is much enhanced, decaying only algebraically as a function

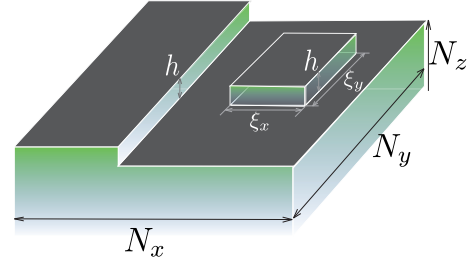


FIG. 1: (Color online) Upper and lower terraces separated by a step of height h are examples of the dark surface of WTI. On the lower terrace is an island formed with the same height.

of the linear dimension of the system.

In contrast to a STI, a WTI can have “dark” surfaces on which no gapless Dirac state appears. Such dark surfaces can be made by cleaving the bulk crystal in the direction specified by the Miller indices $(\nu_1\nu_2\nu_3)$, or equivalently, by placing the surface normally to the “weak vector” $\boldsymbol{\nu} = (\nu_1, \nu_2, \nu_3)$. As a consequence of the existence of these dark surfaces WTI samples can exhibit size effects different from that of a STI of the same shape [8]. Typically, the size effects show *even/odd* feature with respect to the number of layers stacking in the direction of $\boldsymbol{\nu}$. It has also been pointed out that a WTI is not that weak either against disorder [5, 14, 15]. Here, in this Letter we highlight another striking manifestation of a hidden non-trivial character of the WTI phase. The work is indeed motivated by an experimental discovery of such a WTI and the possibility of cleavage in the plane normal to $\boldsymbol{\nu}$, *i.e.*, realizing a dark surface of WTI [16].

We start by demonstrating that a closed loop of perfectly conducting channel (PCC) is formed at the periphery of an atomic-layer-thick terrace of height corresponding to an odd number of atomic layers formed on a dark surface of WTI. Experimental observation of such atomic-scale terraces formed on an otherwise flat surface of a topological insulator by STM measurements have been also reported previously [17].

Let us consider the following standard Wilson-Dirac type effective Hamiltonian for 3D topological insulators,

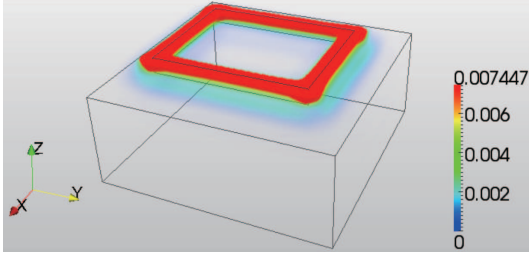


FIG. 2: (Color online) A pseudo-gapless 1D mode emergent along the periphery of an island. The island has a size of $\xi_x \times \xi_y = 9 \times 11$, and an altitude $h = 1$. The systems's sizes are $N_x = N_y = 16, N_z = 7$.

here implemented on the cubic lattice as

$$\begin{aligned} H_{\text{bulk}} &= A\tau_x\sigma_\mu \sin k_\mu + \tau_z m(\mathbf{k}), \\ m(\mathbf{k}) &= m_0 + 2m_{2\mu}(1 - \cos k_\mu), \end{aligned} \quad (1)$$

where two types of Pauli matrices σ and τ represent real and orbital spins, and $\mu = x, y, z$. The parameter A represents the strength of normal hopping, and determines the aperture of the surface Dirac cone. To realize a WTI with a specific choice of weak indices $\nu = (0, 0, 1)$, we choose the mass parameters to be anisotropic. In the following demonstrations they are chosen such that $m_0 = -1$, $m_{2x} = m_{2y} = 0.5$ and $m_{2z} = 0.1$ in units of the hopping parameter A [8]. In the actual simulations on-site random potential is also introduced as in Ref. [15]. The global shape of the sample is also assumed to be tetragonal apart from terraces and islands; see below, i.e., the underlying lattice is, unless otherwise mentioned, terminated in all the three (x -, y - and z -) directions, and in principle could accommodate a surface state on all of its tetragonal faces, but because of the weak vector pointing to the \hat{z} -direction that excludes Dirac cones from the surfaces normal to this direction, the system exhibits pseudo-gapless surface states only on the four side surfaces.

Let us now consider a situation in which the top surface is not completely flat, showing either atomic-scale terrace-like step structures or an isolated island-shaped region as depicted in Fig. 1. When the surface is normal to ν , the vertical wall of this step structure is parallel to ν , on which one can hypothesize formation of gapless 2D surface states (two Dirac cones). Then, of course, contributions from these two Dirac cones must be superposed to cope with the boundary condition that the wave function is not allowed to leak onto the dark terraces [8].

Fig. 2 and Fig. 3 (a) demonstrate that there appears indeed a pair of 1D modes almost localized at the periphery of such a terrace- or an island-shaped region, when its height h (measured in units of the lattice constant) is odd ($h = 1, 3, 5, \dots$). These 1D modes are, in contrast to 2D surface states, immune to backward scattering as a consequence of their helical nature, and realize an example of what is often called “perfectly conducting channels”

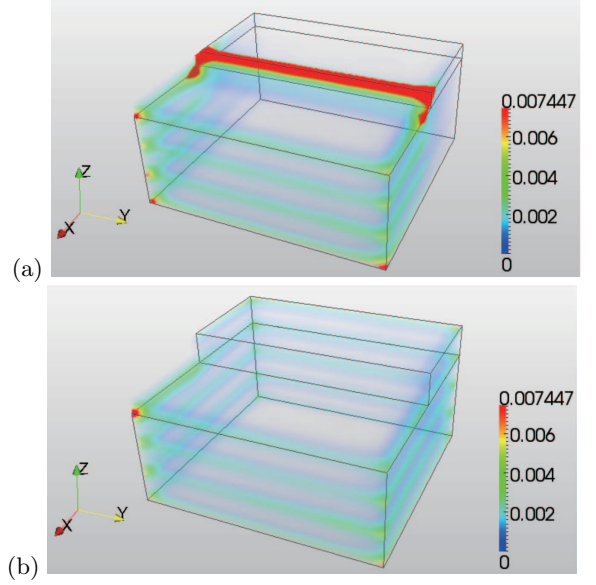


FIG. 3: (Color online) Profile of the lowest energy wave function in atomic-scale terraces of a WTI. (a) When $h = 1$, 1D modes appear at the edge of the terrace. (b) when $h = 2$, the wave function has a vanishing amplitude along the edge of the terraces. $N_x = N_y = 16, N_z = 7$.

[18]. The wave functions associated with these 1D channels shown in Fig. 2 and Fig. 3 (a) are barely influenced by the presence of weak disorder; here, the strength of disorder is chosen as $W/A = 1$ in the notation of [8]. The above numerical simulations have been performed in systems of a rather simple shape of the island and of the terrace. While, the appearance of a 1D PCC is considered to be generic, and equally applicable to systems that are smoothly connected to the present one as far as h is odd.

If h is even, the situation is much different as a result of the *even/odd* feature of finite-size gap generation characteristic to the surface of WTI [8]. This *even/odd* feature is associated with the fact that a WTI is sometimes described as stacked layers of 2D quantum spin Hall states, each exhibiting a pair of helical edge modes. These helical edge modes, when stacked to form a helical surface state, tend to couple into gapped pairs, leaving only a single gapless channel when the number of stacked layers is odd. A more quantitative $\mathbf{k} \cdot \mathbf{p}$ -type argument developed in Ref. [8] suggests when applied to the terrace- or island-shaped region that the pseudo-zero-energy states acquire a finite energy, $E_{\pm} = \pm \frac{A}{2(h+1)}\pi$, when its height h is even. Here, the pseudo-gapless 1D helical modes are completely kicked out of the low-energy spectrum [see Fig. 3 (b)]. The case of a two-story ($h = 2$) terrace is an example in which this (parity of) h -dependent size effect is most accentuated, giving rise to a huge finite-size correction to the energy of pseudo-zero modes as, $E_{\pm} = \pm \frac{A}{6}\pi$, i.e., on the order of 1 in units of A .

The protected 1D modes emergent when h is odd, typi-

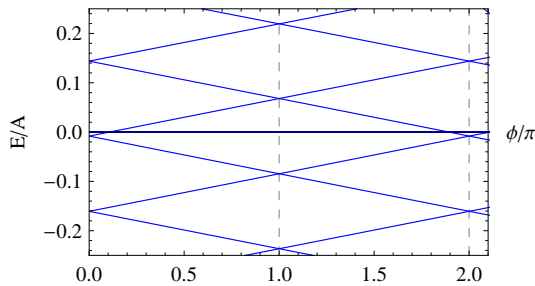


FIG. 4: (Color online) A numerical experiment: verification of the perfectly conducting character of the 1D channels circulating the periphery of the island (case of $h = 1$). The spectrum of the 1D modes is plotted against the inserted flux ϕ .

cally one, are not entirely immune to finite-size gap opening, but of a different, less destructive type. On one hand, these counter propagating modes are always in the opposite spin state (spin-to-momentum locking), and this very fact makes them immune to backward scattering by the impurities. While, on the other hand, the quantization axis of these spins can and does indeed rotate as an electron propagates along this circular 1D orbital, in such a way that this quantization axis is normal to the tangent of this 1D orbital (spin-to-surface locking); a situation analogous to the one occurring at a cylindrical surface of STI [10–12]. As a result, while an electron revolves once around a circular orbit, its spin also performs a complete 2π rotation, altering the orbital part of the boundary condition from periodic to anti-periodic. This leads, tracing exactly the same path as in the case of the half-odd integral quantization of the orbital angular momentum L_z in a cylindrical STI [8, 12], to a finite-size correction $E_{\pm} = \pm \frac{\tilde{A}}{s}\pi$, where \tilde{A} is a constant of order A , and $s = 4\xi$ is the circumference of the island.

To double check that the pseudo-gapless 1D modes in the case of h being odd realize indeed a single pair of perfectly conducting channels, and that they are immune to backward scattering by the impurity, we have performed the following numerical experiment. In a situation as depicted in Fig. 2, in which a 1D ring-shaped distribution of the wave function is realized along the periphery of an island, we gradually introduce a magnetic flux tube (of magnitude Φ) threading the island such that ideally the flux would not touch the electron. The boundary condition on the side surfaces are here chosen to be doubly periodic, *i.e.*, a slab geometry is employed to avoid 2D states on the side surfaces. Fig. 4 depicts the result of such a numerical experiment in which the spectrum of the 1D states is plotted against ϕ . Here, $\phi = 2\pi \frac{\Phi}{\Phi_0}$ is an Aharonov-Bohm phase associated with the external flux Φ measured in units of the flux quantum Φ_0 . One can clearly observe that (i) the spectrum is doubly degenerate at $\phi = 0$ and at $\phi = \pi$, (ii) as ϕ is introduced,

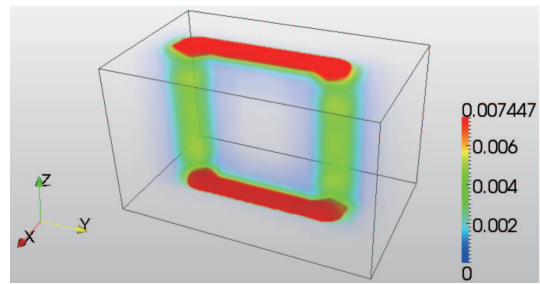


FIG. 5: (Color online) A finite segment of 1D gapless modes penetrating into the bulk WTI at the ends of the segment along a screw dislocation line with $\mathbf{b} = b\mathbf{\hat{z}}$ ($b = \pm 1$). The two dislocation lines are separated by a distance of $\zeta = 8$. $N_x = 16, N_y = N_z = 10$.

say at $\phi = 0$, this two-fold degeneracy is lifted in such a way that one state is shifted upward, and the other downward, indicating the existence of counter propagating channels. Note also that (iii) at $\phi = 0$ and at $\phi = \pi$, the pairs are swapped, and (iv) the ϕ -dependence of each spectrum is almost perfectly linear. These features are perfectly in accordance with our hypothesis that a pair of 1D helical modes are formed at the periphery of the island.

The spectrum of the 1D helical modes in the presence of a flux Φ can be written most generally as

$$E_n^{(\pm)}(\phi) = \pm \tilde{A} \frac{\pi}{s} \left(n - \frac{1}{2} - \frac{\phi}{2\pi} \right) + \Delta E, \quad (2)$$

where ΔE represents a global shift of the spectrum associated with the breaking of the particle-hole symmetry due to on-site random potentials. At $\phi = 0$, the two-fold degeneracy of the spectrum occurs such that $E_n^{(+)}(0) = E_{-n+1}^{(-)}(0)$, while at $\phi = \pi$, after these partners are shifted in the opposite directions, perfectly linearly to ϕ , each state gets paired again but with a different partner such that $E_n^{(+)}(\pi) = E_{-n}^{(-)}(\pi)$, *i.e.*, in such a way that the relative ordering of the partners is shifted by one [19].

We have seen so far examples in which pseudo-gapless protected 1D modes appear on a dark surface of WTI, forming either a closed loop, *e.g.*, at the periphery of an island, or a line, *e.g.*, at the boundary of two terraces, crossing the dark surface completely, only to merge with a 2D side-surface state at both ends. In the remainder of this Letter we focus on another type of 1D modes emergent on the dark surface, typically as a *finite segment of a line* of length ζ . We demonstrate that this type of 1D modes are associated with the presence of dislocation lines in the crystal, and indeed the two ends of the segment coincide with the termination of a dislocation line at the dark surface (see Fig. 5).

To convince oneself that this is certainly the case let us first turn around the argument in the following way. Recall that a pair of gapless 1D helical modes are in-

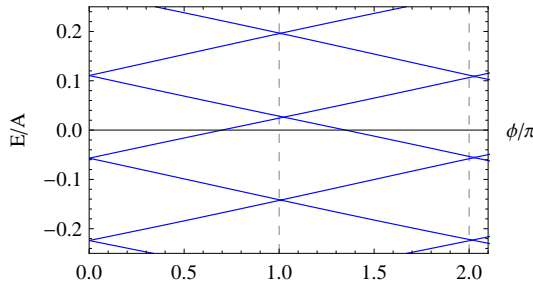


FIG. 6: (Color online) The “flux experiment” applied to a configuration with a pair of screw dislocation lines.

duced along a dislocation line introduced in the bulk WTI [4, 7], when the Burgers vector \mathbf{b} specifying the dislocation satisfies the relation, $\mathbf{b} \cdot \mathbf{M} = \pi \bmod 2\pi$, where the vector \mathbf{M} is defined in terms of the weak indices and the three reciprocal lattice vectors $\mathbf{G}_1, \mathbf{G}_2, \mathbf{G}_3$ as $\mathbf{M} = \frac{1}{2}(\nu_1 \mathbf{G}_1 + \nu_2 \mathbf{G}_2 + \nu_3 \mathbf{G}_3)$. The question to be addressed here can then be reformulated in the following way. What happens to the single pair of gapless 1D helical modes that emerges along a dislocation line, when the dislocation is terminated at a dark surface of WTI? In any realistic setup it is natural to assume that a dislocation line is terminated at the surface of the sample at both ends, unless it forms a closed loop. Here, we consider a dislocation line terminated by the two *dark* surfaces, such as the ones on the top and on the bottom (see Fig. 5). Since these dark surfaces are normal to $\boldsymbol{\nu}$, the condition for the existence of gapless 1D helical modes is satisfied, only when the introduced dislocation is a *screw* dislocation with a dislocation line parallel to \mathbf{b} . When such a screw dislocation is terminated at the surface of a sample, it necessarily accompanies a mismatch of atomic layers by a magnitude of $b = |\mathbf{b}|$, forming typically a step structure, analogous to the one that appears between the two terraces.

Let us come back to the original point of view in which our focus is on a finite segment of the 1D helical modes emergent on the dark surface. Notice that a single pair of such Dirac states cannot be confined, in principle, in a finite segment (Klein tunneling). The only way (out) for such a segment of 1D modes to appear on the dark surface is that it pair-annihilates with another 1D helical modes along a dislocation line that terminates at the dark surface. This is explicitly demonstrated in Fig. 5.

The last question to be addressed is whether these continuous 1D channels partly hosted by a dislocation line, combined with a segment of 1D modes on the dark surface realize also a perfectly conducting channel. For this purpose we have performed a numerical experiment, analogous to the one for the island geometry, but here, the flux tube is inserted between the two dislocation lines. In Fig. 6 one can clearly recognize the four characteristic features supporting the formation of a pair of 1D helical

modes observed in the case of the island. Here, in the present geometry this confirms that different parts of the helical modes, one on the dark surface, and the other along a dislocation line, are indeed smoothly connected to form a 1D perfectly conducting channel. Here, s in Eq. (2) is given by $s = 2(\zeta + N_z)$, the circumference of the 1D channel.

A single pair of pseudo-gapless 1D helical modes also appears along a dislocation line inserted in a STI. However, when the pair is hosted by a STI, it necessarily terminates in the “sea” of the single-cone Dirac state at the surface where surface sensitive measurements are applicable. Here, we have provided a more experimentally feasible situation to detect a dislocation solely from information on the surface, by predicting that *termination* of a 1D perfectly conducting channel on the dark surface of WTI accompanies a screw dislocation line in the bulk host crystal that terminates at the dark surface.

KI acknowledges M. Kanou and T. Sasagawa for stimulating discussions. KI and YT are supported by KAKENHI; KI by the “Topological Quantum Phenomena” (No. 23103511), and YT by a Grant-in-Aid for Scientific Research (C) (No. 24540375).

-
- [1] L. Fu, C. L. Kane, and E. J. Mele, Phys. Rev. Lett. **98**, 106803 (2007).
 - [2] J. E. Moore and L. Balents, Phys. Rev. B **75**, 121306 (2007).
 - [3] R. Roy, Phys. Rev. B **79**, 195322 (2009).
 - [4] K.-I. Imura, Y. Takane, and A. Tanaka, Phys. Rev. B **84**, 035443 (2011).
 - [5] Z. Ringel, Y. E. Kraus, and A. Stern, Phys. Rev. B **86**, 045102 (2012).
 - [6] L. Fu and C. L. Kane, Phys. Rev. B **76**, 045302 (2007).
 - [7] Y. Ran, Y. Zhang, and A. Vishwanath, Nature Physics **5**, 298 (2009).
 - [8] K.-I. Imura, M. Okamoto, Y. Yoshimura, Y. Takane, and T. Ohtsuki, Phys. Rev. B **86**, 245436 (2012).
 - [9] Y. Zhang, K. He, C.-Z. Chang, C.-L. Song, L.-L. Wang, X. Chen, J.-F. Jia, Z. Fang, X. Dai, W.-Y. Shan, et al., Nature Physics **6**, 584 (2010).
 - [10] Y. Zhang and A. Vishwanath, Phys. Rev. Lett. **105**, 206601 (2010).
 - [11] J. H. Bardarson, P. W. Brouwer, and J. E. Moore, Phys. Rev. Lett. **105**, 156803 (2010).
 - [12] K.-I. Imura, Y. Takane, and A. Tanaka, Phys. Rev. B **84**, 195406 (2011).
 - [13] K.-I. Imura, Y. Yoshimura, Y. Takane, and T. Fukui, Phys. Rev. B **86**, 235119 (2012).
 - [14] R. S. K. Mong, J. H. Bardarson, and J. E. Moore, Phys. Rev. Lett. **108**, 076804 (2012).
 - [15] K. Kobayashi, T. Ohtsuki, and K.-I. Imura, ArXiv e-prints (2012), 1210.4656.
 - [16] M. Kanou and T. Sasagawa, presented at the autumn meeting of the Physical Society of Japan (20aEA-11), Yokohama National University, Sep. 20th, 2012.
 - [17] J. Seo, P. Roushan, H. Beidenkopf, Y. S. Hor, R. J. Cava,

- and A. Yazdani, *Nature* **466**, 343 (2010).
- [18] Y. Takane, *Journal of the Physical Society of Japan* **73**, 2366 (2004).
- [19] K. Nomura, M. Koshino, and S. Ryu, *Phys. Rev. Lett.* **99**, 146806 (2007).